Det Kongelige Danske Videnskabernes Selskab
Matematisk-fysiske Meddelelser, bind **28**, nr. 9

Dan. Mat. Fys. Medd. **28**, no. 9 (1954)

THEORETICAL ANGULAR CORRELATIONS IN ALLOWED BETA TRANSITIONS

BY

O. KOFOED-HANSEN

København
i kommission hos Ejnar Munksgaard
1954

Printed in Denmark.
Bianco Lunos Bogtrykkeri A-S.

The angular distribution in beta decay is usually expressed in terms of the beta particle energy and the angle between the directions of emission of the electron and the neutrino. In the present paper, this distribution is transformed into the distribution function for any two of the observable variables, viz. the beta energy, the recoil energy, and the angle between the direction of emission of the recoil and the electron.

Introduction.

In beta transitions, the angular correlation is commonly expressed in terms of the beta particle energy, E, and the angle, θ, between the directions of the momentum of the electron, p, and that of the neutrino, q.

For allowed transitions, $\Delta J = \begin{cases} 0 \\ \pm 1 \end{cases}$ (no), this correlation is given by the probability distribution for E and θ[1), 2)]

$$\left.\begin{aligned} &P(E,\theta)\, dE\, d\Omega_\theta \\ &= F(Z,E)\, pEq^2\, [1 + (b/E) + (ap/E)\cos\theta]\, dE\, d\Omega_\theta , \end{aligned}\right\} \quad (1)$$

where $d\Omega_\theta$ is a solid angle interval around θ; $F(Z,E)$ is the Coulomb correction as a function of E and the charge Z of the recoil, and

$$b = 2\sqrt{1-(\alpha Z)^2}\, \frac{g_S g_V \left|\int 1\right|^2 + g_T g_A \left|\int \vec{\sigma}\right|^2}{(g_S^2+g_V^2)\left|\int 1\right|^2 + (g_T^2+g_A^2)\left|\int \vec{\sigma}\right|^2}, \quad (2)$$

where α is the fine structure constant, and the g's are the relative coupling constants for scalar (S), vector (V), tensor (T), and axial vector (A) couplings, respectively. Furthermore, $\left|\int 1\right|^2$ is the square of the nuclear matrix element for the Fermi interactions, and $\left|\int \vec{\sigma}\right|^2$ is the corresponding square for the Gamow-Teller interactions. Finally,

$$a = \frac{(g_V^2-g_S^2)\left|\int 1\right|^2 + \frac{1}{3}(g_T^2-g_A^2)\left|\int \vec{\sigma}\right|^2}{(g_S^2+g_V^2)\left|\int 1\right|^2 + (g_T^2-g_A^2)\left|\vec{\sigma}\right|^2}. \quad (3)$$

The units are as usual in beta decay: $\hbar = 1$, $c = 1$, and $m = 1$. The pseudoscalar interaction has been omitted, since it contributes to allowed transitions only with higher order terms[3].

The expression (1) is mathematically convenient, since E and θ may vary independently in the intervals $1 \leq E \leq E_0$ and $0 \leq \theta \leq \pi$, respectively, and since E and θ completely determine the momentum triangle (apart from orientation in space[4]). This is a result of the fact that the neutrino rest mass has been equated to zero, as can be seen from the conservation of energy and momentum, which shows that E, θ determines one and only one value of q.

Physically, however, (1) is less convenient because it refers to the neutrino which, at the present time, cannot be observed in angular correlation experiments. The transformation of the angular correlation (1) into distribution functions for any two of the three measurable quantities p, φ, and r, where r is the recoil momentum and φ the angle between the directions of r and p, is straightforward. In the present paper, it is the intention to give the three distribution functions corresponding to (1) for the three pairs of variables (E, r), (E, φ), and (r, φ) for reference use.

The essential questions which arise are, firstly, inside which area can the variables so chosen vary and, secondly, do the variables determine the momentum triangle completely so that the transformation establishes a one to one correspondence between the old and the new variables.

The (E, r) Distribution.

For the transformation of (1), the guiding relations are the conservation laws of energy and momentum given by

$$E + q = E_0, \tag{4}$$

$$p^2 + q^2 + 2\,pq \cos\theta = r^2, \tag{5}$$

which are valid when the recoil mass is considered infinite. By differentiation of θ with respect to r, (5) gives

$$|\sin\theta\, d\theta| = 2\, d\Omega_\theta = \frac{r}{pq}\, dr. \tag{6}$$

However, in the case of the (E, r) distribution, one has to remember that E and r cannot vary independently inside the intervals $0 \leq r \leq p_0$, $1 \leq E \leq E_0$ with

$$p_0 = \sqrt{E_0^2 - 1}.$$

We find from (5), for a fixed value of r,

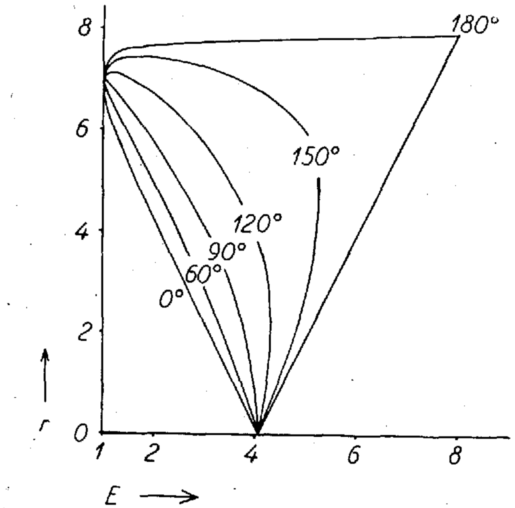

Fig. 1. Permitted area in the (E, r) plane for $E_0 = 8$. In the diagram, curves are drawn for constant values of φ referring to relation (10).

$$\frac{(E_0 - r)^2 + 1}{2\,(E_0 - r)} \leq E \leq \frac{(E_0 + r)^2 + 1}{2\,(E_0 + r)} \tag{8}$$

or, correspondingly, for a fixed value of E,

$$|p - q| \leq r \leq |p + q|, \tag{9}$$

where $p = \sqrt{E^2 - 1}$ and q is given by (4). Relations (8) and (9) are illustrated in Fig. 1 for a definite numerical example.

On the other hand, given values of E and r inside the permitted area determined by (8) and (9) give one and only one value for the angle φ inside the interval $0 \leq \varphi \leq \pi$. This follows from the conservation of momentum, written in terms of E, r and φ,

$$\cos\varphi = \frac{q^2 - p^2 - r^2}{2\,pr}. \tag{10}$$

Relation (10) is also illustrated in Fig. 1. Two trivial excep-

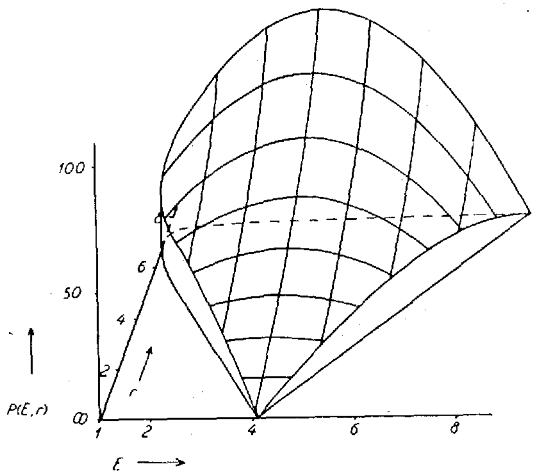

Fig. 2. (E, r) distribution for $E_0 = 8$, $Z = 0$, and pure tensor interaction.

tions to the unique determination of φ exist, namely, all φ values meet in the two points

$$(E, r) = \left(\frac{E_0^2 + 1}{2\,E_0}, 0\right), \tag{11}$$

corresponding to $p = q$, and

$$(E, r) = (0, E_0 - 1), \tag{12}$$

corresponding to $r = q^{\max} = E_0 - 1$. The limiting curves $r = p - q$, $(p > q)$ and $r = q + p$ correspond to $\varphi = \pi$, and the limiting curve $r = q - p$, $(p < q)$ corresponds to $\varphi = 0$.

The transformation from (1) to the (E, r) distribution can thus be carried out immediately, and one finds

$$\left.\begin{aligned} &P(E, r)\, dE\, dr \\ &= \frac{1}{2} F(Z, E)\left[rEq + brq + r\frac{a}{2}(r^2 - p^2 - q^2)\right] dE\, dr. \end{aligned}\right\} \tag{13}$$

This distribution function is illustrated in Fig. 2 for pure tensor interaction and $Z = 0$, and in Fig. 3 for pure axial vector interaction and $Z = 0$, in both cases for the same numerical example as chosen in Fig. 1.

In Figs. 2 and 3, and from formula (13), one sees that the (E, r) distribution is extremely simple, except for the complicated cut-off introduced by (8) or (9). For fixed values of r, the E distributions are parabolic and symmetric around $q = E = E_0/2$,

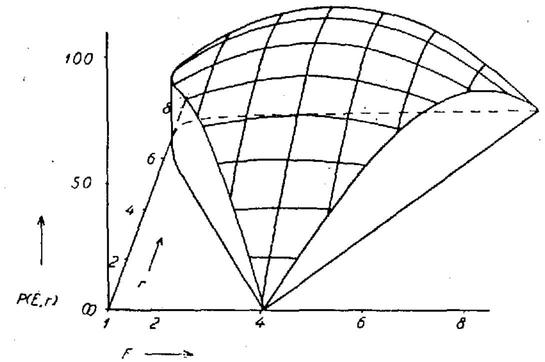

Fig. 3. (E, r) distribution for $E_0 = 8$, $Z = 0$, and pure axial vector interaction.

apart from the Coulomb correction. For fixed values of E, the r distributions are polynomials of the 3rd order in r, the entire expression consisting of r multiplied into a parabolic expression in r. The energy distribution for the kinetic energy R of the recoil is thus even simpler; we can write

$$\mathrm{R} = r^2/(2\,M) \tag{14}$$

and get

$$\left.\begin{aligned} &P(E, R)\, dE\, dR \\ &= \frac{M}{2} F(Z, E)\left[Eq + bq + \frac{a}{2}(2\,MR - p^2 - q^2)\right] dE\, dR. \end{aligned}\right\} \tag{15}$$

For fixed R values, this equation shows the same general shapes of the β-energy distribution as (13) and give, for fixed E values, a linear dependence on R.

The (E, φ) Distribution[5].

While the (E, θ) distribution and, in some respects, the (E, r) distribution are very simple, this is not the case for the (E, φ) and (r, φ) distributions. This fact is of course entirely due to the conservation laws and is apparent from (10) and the corresponding curves for constant φ values in Fig. 1. It is immediately

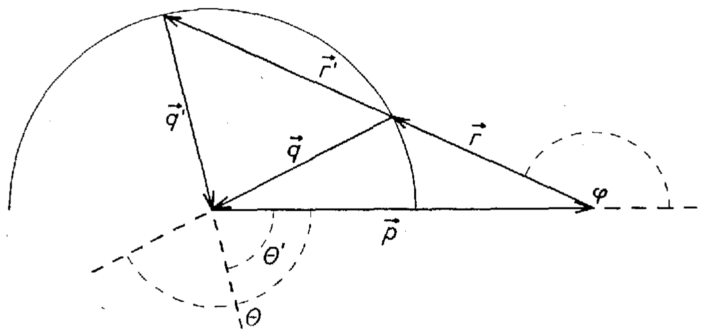

Fig. 4. Momentum triangle for $E_0 = 8$, $E = 5$, and $q = 3$. For a given value of φ, two solutions of r are obtained, viz., $\vec{r}$ and $\vec{r}'$.

seen that, when $p > q$, i. e., $E > \frac{E_0^2 + 1}{2E_0}$, and $\frac{\pi}{2} \leq \varphi \leq \pi$, given values of E and φ lead to two solutions for r. This finds of course also a simple geometrical interpretation, as illustrated by the momentum triangle shown in Fig. 4.

It is also evident that a given value of $E > \frac{E_0^2+1}{2E_0}$ only permits φ to vary between $\varphi' \leq \varphi \leq \pi$, where

$$\sin\varphi' = q/p, \quad \frac{\pi}{2} \leq \varphi' \leq \pi, \tag{16}$$

or, correspondingly, that a given value of $\varphi' \geq \frac{\pi}{2}$ permits as an interval for E

$$1 \leq E \leq E' = \left\{ \begin{array}{l} \frac{1}{\cos^2\varphi'}\left(E_0 - \sin\varphi' \sqrt{E_0^2 - \cos^2\varphi'}\right) \\ \to \frac{E_0^2+1}{2E_0} \quad \text{for} \quad \varphi' \to \frac{\pi}{2}. \end{array} \right\} \tag{17}$$

We have written down also the limiting value for $\varphi \to \frac{\pi}{2}$. The

formulas (16) and (17) constitute the limiting curves in the E, φ plane. These are illustrated in our specific numerical example in Fig. 5.

The description by our two variables is in this case not complete, as already mentioned. Curves for constant values of

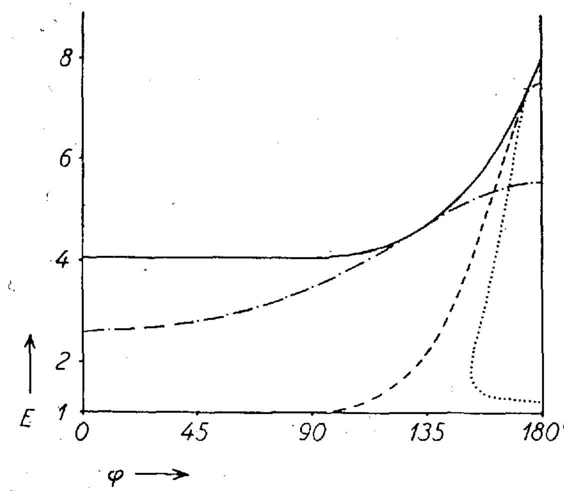

Fig. 5. Permitted area in the (E, φ) plane for $E_0 = 8$ and curves for constant r values.

············	$r = 7.5$
– – – – – – –	$r = 7$
– · – · – ·	$r = 3$.

r intersect in the area $\frac{\pi}{2} \leq \varphi \leq \pi$ and $E > \frac{E_0^2+1}{2E_0}$, as illustrated in Fig. 5. For $r < E_0 - 1$, they extend from $\varphi = 0$ to $\varphi = \pi$, for $r = E_0 - 1$, they extend from $\varphi = \frac{\pi}{2}$ to $\varphi = \pi$, whereas for $r > E_0 - 1$, the curves begin at $\varphi = \pi$ and end at $\varphi = \pi$ again.

When performing the transformation from (13) to the (E, φ) distribution, we clearly have to distinguish between the two cases $p \geq q$ and $p \leq q$.

A: $p \leq q$. We find

$$r = -p\cos\varphi + \sqrt{q^2 - p^2\sin^2\varphi} \tag{18 a}$$

and, correspondingly, by differentiation with respect to φ,

$$\left|\frac{dr}{d\Omega_\varphi}\right| = 2\,p\left(1 - \frac{p\cos\varphi}{\sqrt{q^2 - p^2\sin^2\varphi}}\right). \tag{19 a}$$

Consequently, we find the (E, φ) distribution given by

$$\left.\begin{aligned} P(E,\varphi)\,dE\,d\Omega_\varphi = {} & [pF(Z,E)\left(\sqrt{q^2-p^2\sin^2\varphi} - p\cos\varphi\right)^2\{q(E+b) \\ & - ap\left(p\sin^2\varphi + \cos\varphi\sqrt{q^2-p^2\sin^2\varphi}\right)\}/\sqrt{q^2-p^2\sin^2\varphi}]\,dE\,d\Omega_\varphi, \end{aligned}\right\} \tag{20 a}$$

where $0 \le \varphi \le \pi$.

B: $p \ge q$. We find

$$r = -p\cos \pm \sqrt{q^2 - p^2\sin^2\varphi} \tag{18 b}$$

and, correspondingly, by differentiation,

$$\left|\frac{dr}{d\Omega_\varphi}\right| = 2\,p\left(-\frac{p\cos\varphi}{\sqrt{q^2 - p^2\sin^2\varphi}} \pm 1\right). \tag{19 b}$$

The (E, φ) distribution adds up of two parts, one from each of the solutions to (18b), i. e.,

$$\left.\begin{aligned} P(E,\varphi)\,dE\,d\Omega_\varphi = {} & (20,\text{a}) + [pF(Z,E)\left(\sqrt{q^2-p^2\sin^2\varphi} + p\cos\varphi\right)^2 \\ & \{q(E+b) - ap\left(p\sin^2\varphi - \cos\varphi\sqrt{q^2-p^2\sin^2\varphi}\right)\}/\sqrt{q^2-p^2\sin^2\varphi}]\,dE\,d\Omega_\varphi \end{aligned}\right\} \tag{20 b}$$

$$\left.\begin{aligned} = 2\,pF(Z,E)\,[& \{(q^2+p^2\cos 2\varphi)/\sqrt{q^2-p^2\sin^2\varphi}\}\{q(E+b) - ap^2\sin^2\varphi\} \\ & + 2\,ap^2\cos^2\varphi\sqrt{q^2-p^2\sin^2\varphi}]\,dE\,d\Omega_\varphi, \end{aligned}\right\} \tag{20 c}$$

where $\varphi' \le \varphi \le \pi$. An experimental cut-off of low velocity recoils would affect the two terms in (20b) differently. This is the reason why this intermediate formula is given.

In the limit of $p = q$, both (20a) and (20b) give the following expression for $\frac{\pi}{2} \le \varphi \le \pi$:

$$P(\varphi)\,d\Omega_\varphi = 4\,p^3F\left|\cos\varphi\right|\{(E+b) + ap\cos 2\,\varphi\}\,d\Omega_\varphi; \tag{20 d}$$

for $0 \le \varphi \le \frac{\pi}{2}$, they give $P(\varphi) = 0$.

The distribution functions (20) are illustrated in Figs. 6 for fixed values of E. For $p < q$, the curves are quite regular and extend from $\varphi = 0$ to $\varphi = \pi$. As $p \to q$, the probability for $\varphi < \frac{\pi}{2}$ becomes smaller and smaller relative to the probability

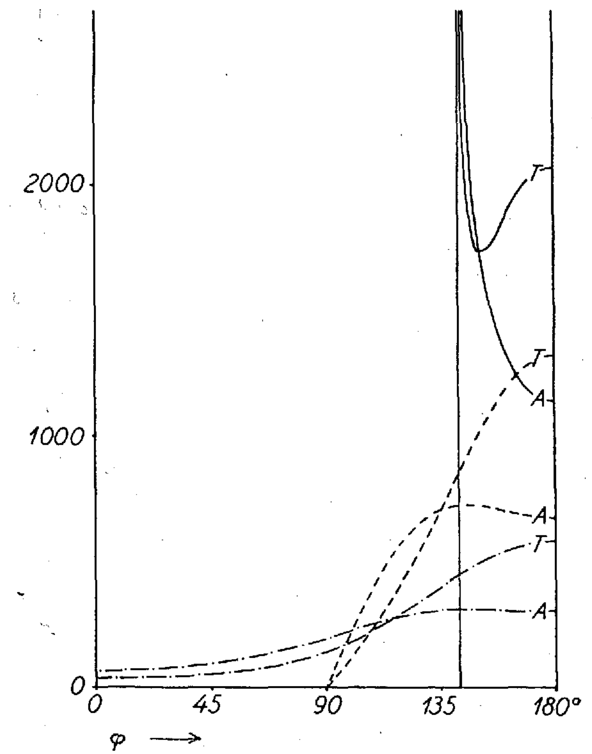

Fig. 6. Relative angular correlations for tensor and axial vector interactions per unit solid angle interval for $E_0 = 8$, $Z = 0$.

— · — · — · $E = 2.79$ $p/q = 0.5$
– – – – – – – – $E = 4.063$ $p = q$
———————— $E = 5.$

for $\varphi > \frac{\pi}{2}$ until, for $p = q$, the probability for $\varphi \le \frac{\pi}{2}$ is zero and the distribution then extends in a regular manner from $\varphi = \frac{\pi}{2}$ to $\varphi = \pi$. For $p > q$, the curves have an integrable singularity at $\varphi = \varphi'$ and extend from $\varphi = \varphi'$ to $\varphi = \pi$. For $p = p_0$, one sees that $\varphi = \pi$, and it should be noted that the limiting value for $p = p_0$, $\varphi = \pi$, is undetermined from formula (20). For values of $p/q < 1$, the curves for T and A interaction intersect at $\mathrm{tg}\,\varphi'' = -q/p$; for $p/q = x < 1$, the curves for T and A interaction intersect at $\varphi'' > \frac{\pi}{2}$, given by $x^2 = \frac{1 + 3\cos 2\varphi''}{(1 + 2\cos 2\varphi'')(1 - \cos 2\varphi'')}$.

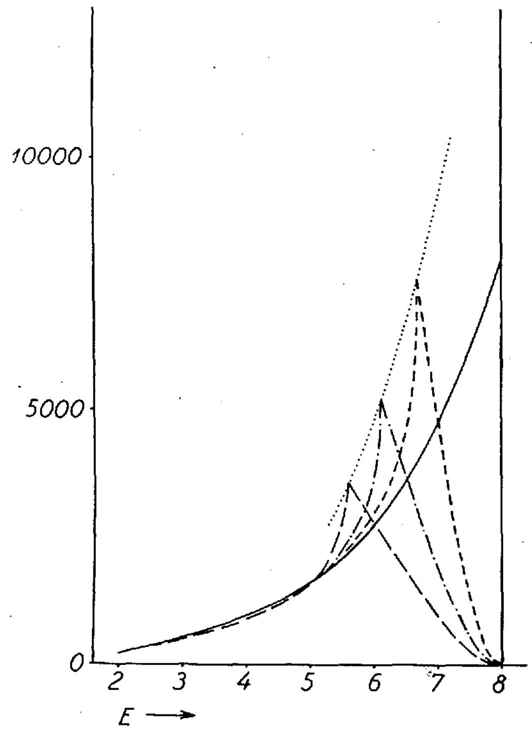

Fig. 7. Beta energy distribution for $\varphi = \pi$ and $E_0 = 8$, $Z = 0$, $b = a = 0$. The curves are normalized per unit interval $d\Omega = \Omega$

———————— infinitely good geometry
- - - - - - - - - $\Omega = 1/100$
— · — · — · $\Omega = 1/40$
— — — — — $\Omega = 1/20$.

This means that for small values of φ the A interaction gives a larger probability than the T interaction; the opposite is the case for large values of φ; the cross-over is at $\varphi = \varphi''$.

Similar considerations apply to the E distributions for fixed values of φ. Let us consider a special case, viz. $\varphi = \pi$. A numerical example is shown in Fig. 7. This curve, however, calls only for physical interest if infinitely good geometry can be obtained. If the instrument permits only a certain resolution as regards the angle, the spectrum (20) has to be integrated over this angular interval. Let us consider an idealized geometry with reception of all particles for $\varphi^* < \varphi < \pi$ and of no particles outside this interval. Let, furthermore, the solid angle be $\Omega = \frac{1}{2}(1 + \cos\varphi^*)$. It then follows that the energy distribution is simply the total beta spectrum from $E = E_0$ down to E' given by (17) with $\varphi = \varphi^*$. At this point, the curve shows a peak and leaves the beta spectrum, approaching at low energies the spectrum for infinitely good geometry for $\varphi = \pi$. Examples of such curves for different values of Ω are also shown in Fig. 7. The peak values lie on the dotted curve which, for $\Omega \rightarrow 0$, approaches the double of the continuous extension of the $\Omega = 0$ curve. This value may be used to define the $P(E_0, \pi)$ value which is undetermined from (20). For comparison with actual experiments[6)*], one has to rely on calculated or measured angular resolution curves which, of course, differ from the simple assumptions made here. It is also necessary to average over the energy resolution for both recoil and beta energy. It should be noted that a misinterpretation of these resolution curves easily may falsify the picture.

The (r, φ) Distribution.

When r and φ are taken as variables, the possible intersection of p and q in the momentum triangle lies on an ellipse, as illustrated in Fig. 8. This figure shows the limiting case of $r = E_0 - 1$, where the ellipse goes through the endpoint of $\vec{r}$, and where angles $\frac{\pi}{2} \leq \varphi \leq \pi$ are permitted. When $r > E_0 - 1$, the ellipse cuts the vector $\vec{r}$, giving two solutions of E for each value of φ. For $r < E_0 - 1$, the vector $\vec{r}$ is entirely surrounded by the ellipse, thus giving only one solution for E for each value of φ. We clearly have to make a distinction between these two cases.

* The author is indebted to Drs. Rustad and Ruby for sending their unpublished experimental data.

The limiting area in the (r, φ) plane is given by

$$\left.\begin{array}{ll} 0 \leq \varphi \leq \pi & \text{for} \quad r < E_0 - 1, \\ \varphi^{+} \leq \varphi \leq \pi & \text{for} \quad r < E_0 - 1, \end{array}\right\} \quad (21)$$

where

$$\sin \varphi^{+} = \frac{E_0^2 - 1 - r^2}{2\, r} \quad \text{and} \quad \frac{\pi}{2} \leq \varphi^{+} \leq \varphi. \quad (22)$$

Equations (21) and (22) lead, in our case, to the picture

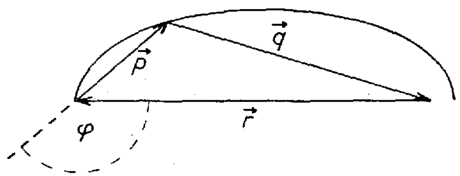

Fig. 8. Momentum triangle for $r = E_0 - 1 = 7$.

shown in Fig. 9. The figure also shows curves for constant values of E and illustrates the existence of two solutions to E for given values of $\varphi > \frac{\pi}{2}$ and $r > E_0 + 1$.

For the (E, r) and the (E, φ) distributions, the Coulomb correction enters quite naturally, since it is expressed as a function of E; this will not be the case when the variables are r and φ. In this case, it is therefore natural to write down the distribution function implicitly as a function of r and φ through expressions for $E = E(r, \varphi)$. We distinguish between the two cases

A: $r < E_0 - 1$. We then find

$$E = \frac{E_0 (E_0^2 + 1 - r^2) - r \cos \varphi \sqrt{(E_0^2 - 1 - r^2)^2 - 4 r^2 \sin^2 \varphi}}{2 (E_0^2 - r^2 \cos^2 \varphi)} \quad (23\,\text{a})$$

and, correspondingly, by differentiation directly of (23a) or implicitly of (10),

$$\left.\begin{array}{l} \left| \dfrac{dE}{d\Omega_\varphi} \right| = \dfrac{2 p^2 r}{E_0 p + E r \cos \varphi} \\ \qquad = \dfrac{4 p^2 r}{\sqrt{(E_0^2 - 1 - r^2)^2 - 4 r^2 \sin^2 \varphi}} \end{array}\right\} \quad (24\,\text{a})$$

which, inserted in (13), gives the (r, φ) distribution

$$\left.\begin{array}{l} P(r, \varphi)\, dr\, d\Omega \\ = F(Z, E) \left[rEq + brq + \dfrac{a}{2} r (r^2 - p^2 - q^2) \right] \dfrac{p^2 r}{E_0 p + E r \cos \varphi}\, dr\, d\Omega_\varphi. \end{array}\right\} \quad (25\text{a})$$

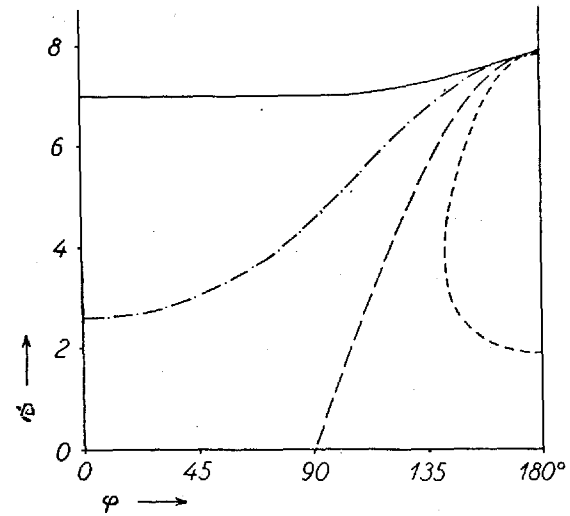

Fig. 9. Limiting area in the (r, φ) plane for $E_0 = 8$. Curves for constant values of E are given.

— · — · — · $E = 2.77$
— — — — — $E = (E_0^2 + 1)/(2\, E_0)$
- - - - - - - - - $E = 5.$

B: $r > E_0 - 1$. We then find

$$\left.\begin{array}{l} E_1 \\ E_2 \end{array}\right\} = \frac{E_0 (E_0^2 + 1 - r^2) \mp r \cos \varphi \sqrt{(E_0^2 - 1 - r^2)^2 - 4 r^2 \sin^2 \varphi}}{2 (E_0^2 - r^2 \cos^2 \varphi)} \quad (23\text{b})$$

and, by differentiation,

$$\left.\begin{array}{l} \left| \dfrac{dE}{d\Omega_\varphi} \right| = \pm \dfrac{2 p^2 r}{E_0 p + E r \cos \varphi} \\ \qquad = \dfrac{4 p^2 r}{\sqrt{(E_0^2 - 1 - r^2)^2 - 4 r^2 \sin^2 \varphi}}. \end{array}\right\} \quad (24\,\text{b})$$

Consequently, one obtains for the (r, φ) distribution

$$P(r,\varphi)\,dr\,d\Omega_\varphi = \left\{F(Z,E_1)\left[rE_1q_1+brq_1+\frac{a}{2}r(r^2-p_1^2-q_1^2)\right]p_1^2 + F(Z,E_2)\left[rE_2q_2+brq_2+\frac{a}{2}r(r^2-p_2^2-q_2^2)\right]p_2^2\right\} \frac{2\,r\,dr\,d\Omega_\varphi}{\sqrt{(E_0^2-1-r^2)^2-4\,r^2\sin^2\varphi}}. \qquad (25\,\text{b})$$

The discussion of these functions (25) is very similar to that of (20). For $r < E_0 - 1$, the curves are regular and, for $r > E_0 - 1$, an integrable singularity appears at $\varphi = \varphi^+$. The two distribution functions (25) both lead, in the limiting case $r = E_0 - 1$, to the expression

$$P(\varphi)\,d\Omega_\varphi = F(Z,E_3) \left[E_3q_3+bq_3+\frac{a}{2}\left\{(E_0-1)^2-p_3^2-q_3^2\right\}\right]\frac{p_3^2(E_0-1)}{|\cos\varphi|} \qquad (25\,\text{c})$$

with

$$E_3 = \frac{E_0^2+(E_0-1)^2\cos^2\varphi}{E_0^2-(E_0-1)^2\cos^2\varphi} \qquad (23\,\text{c})$$

for $\frac{\pi}{2} \le \varphi \le \pi$. For $0 \le \varphi \le \frac{\pi}{2}$, they lead to $P(\varphi) = 0$.

The total r distribution can be obtained from (13) by an integration over E between the limits (8). In the $Z = 0$, $b = 0$ approximation, the result has been given previously[7]. The total φ distribution can be found by integration of (20) or (25). This integration leads to very complicated integrals. Numerical calculations have been carried out for the neutron decay[5), 8)].*

The Influence of the Recoil.

It seems of some interest to study the effects which occur when the kinetic energy of the recoil is not neglected in the conservation of energy (4). We then find

$$E_0 = E + q + r^2/2\,m_R, \qquad (26\,\text{a})$$

where m_R is the recoil mass. If we include the rest mass in the recoil energy $\mathcal{R}$, we get the relativistic expression

* After the conclusion of this paper, the author has received an article by M. E. Rose (O.R.N.L. 1591, 1953) which deals with methods of calculation for the total distribution in certain limits.

$$M = E + \mathcal{R} + q = E_1 + E_2 + E_3, \qquad (26\,\text{b})$$

where M is the mass of the mother nucleus.

Here, it should be kept in mind that the phase space factor

$$rEq\,dE\,dr = E_1E_2E_3\,dE_1\,dE_2 \qquad (27)$$

in (13) has the exact relativistic form when E_3 is inserted from (26 b)[9] and the limiting curves in the (E_1, E_2) plane are taken from formula (6) of reference 9. This formula leads to (8) and (9) apart from terms of the order of E_0/M.

The angular distributions must therefore be divided into this phase space factor and the matrix element factor, and the effect of the neglect of the recoil in (26 a) has to be considered separately for these two factors and for the transformations (19) and (24). The effect on the two first factors is the same as for allowed beta spectra, and only the effect on the transformations need to be considered here. Let us consider a transition in which the mother nucleus of mass M disintegrates into three particles of mass m_1, m_2, and $m_3 = 0$. We have then to distinguish between two cases as follows.

A: $$E_1 < \frac{(M-m_2)^2+m_1^2}{2(M-m_1)}.$$

Here, the angle θ_{12} between the momenta p_1 and p_2 may vary independently between the limits $0 < \theta_{12} \le \pi$.

B: $$E_1 > \frac{(M-m_2)^2+m_1^2}{2(M-m_1)}.$$

In this case, we have $\theta'_{12} \le \theta_{12} \le \pi$, where θ'_{12} is given by

$$\sin\theta'_{12} = \frac{M(E_1^{\max}-E_1)}{m_2p_1}; \quad \frac{\pi}{2} \le \theta'_{12} \le \pi. \qquad (28)$$

When terms of the order of E_0/M are neglected, (28) leads to (16) and (22).

In case A, we find the upper sign and, in case B, both signs in

$$p_2 = \frac{-p_1\cos\theta_{12}\left[M(E_1^{\max}-E_1)+m_2^2\right] \pm (M-E_1)\sqrt{M^2(E_1^{\max}-E_1)^2-m_2^2p_1^2\sin^2\theta_{12}}}{\left[(M-E_1)^2-p_1^2\cos^2\theta_{12}\right]} \qquad (29)$$

and

$$E_2 = \frac{(M-E_1)\left[M(E_1^{\max}-E_1)+m_2^2\right] \mp p_1 \cos\theta_{12} \sqrt{M^2(E_1^{\max}-E_1)^2 - m_2^2 p_1^2 \sin^2\theta_{12}}}{\left[(M-E_1)^2 - p_1^2\cos^2\theta_{12}\right]} \quad (30)$$

(29) and (30) correspond to (18) and (23) in the usual limit. By squaring E_2 and p_2, and subtracting, it is easily seen that the result is m_2^2, provided the signs are kept in the order given in (29) and (30).

Formula (10) is also valid relativistically and may now be written in the form

$$2\, p_1 p_2 \cos\theta_{12} = p_3^2 - p_1^2 - p_2^2 \quad (31)$$

which, by differentiation, leads to

$$\begin{aligned} \frac{dp_2}{d\Omega_{\theta_{12}}} &= \frac{2\, p_1 p_2 E_2}{(M-E_1)\, p_2 + E_2 p_1 \cos\theta_{12}} \\ &= \frac{2\, p_1 p_2 E_2}{\pm\sqrt{M^2(E_1^{\max}-E_1)^2 - m_2^2 p_1^2 \sin^2\theta_{12}}} \end{aligned} \quad (32)$$

which shows the same general features as (19) and (24) and leads to singularities in the (E_1, θ_{12}) distributions when (28) is fulfilled. Formula (19) is obtained from (32) in the limit $m_2 = E_2 = M$, and (24) is obtained from (32) directly by inserting $2\,ME_1 = r^2$, i. e. in the limit $m_1 = M$. The effect of the recoil is therefore a small shift in the position of the singularities and then, if this shift is neglected, i. e., if (20) or (25) is compared with the true distribution function for fixed values of the square roots in (19), (24), and (32), the changes are of the order of magnitude E_0/M, only.

The author is indebted to Professor NIELS BOHR and to the Ole Römer Foundation for financial support.

Institute for Theoretical Physics,
University of Copenhagen,
Denmark.

References.

1. E. GREULING and M. L. MEEKS, Phys. Rev. **82**, 531 (1951).
   L. C. BIEDENHARN and M. E. ROSE, Rev. Mod. Phys. **25**, 729 (1953).
2. S. E. DEGROOT and H. A. TOLHOEK, Physica **16**, 456 (1950).
3. G. ALAGA, O. KOFOED-HANSEN and A. WINTHER, Dan. Mat. Fys. Medd. **28**, no. 3 (1953).
4. H. A. TOLHOEK, Thesis, Utrecht (1951).
5. REYNOLDS, BIEDENHARN and BEARD, Oak Ridge Nat. Lab., Report O.R.N.L., 1444.
6. J. S. ALLEN and W. K. JENTSCHKE, Phys. Rev. **89**, 902 (1953).
   M. B. RUSTAD and S. L. RUBY, Phys. Rev. **89**, 880 (1953).
7. O. KOFOED-HANSEN, Phys. Rev. **74**, 1785 (1948).
8. T. KOTANI, H. TAKEBE, M. UMEZAWA and Y. YAMAGUCHI, Prog. Theor. Phys. **7**, 469 (1952); **8**, 1411 (1952).
9. O. KOFOED-HANSEN, Phil. Mag. **42**, 1411 (1951).

Indleveret til selskabet den 15. januar 1954.
Færdig fra trykkeriet den 26. juni 1954.